THE JOURNAL OF BIOLOGICAL CHEMISTRY VOL. 285, NO. 9, pp. 6670–6680, February 26, 2010


# Phosphorylation-dependent Activation of Peroxisome Proliferator Protein PEX11 Controls Peroxisome Abundance*[S]

Received for publication, December 14, 2009, and in revised form, December 21, 2009 Published, JBC Papers in Press, December 22, 2009, DOI 10.1074/jbc.M109.094805

**Barbara Knoblach and Richard A. Rachubinski**[1]

*From the Department of Cell Biology, University of Alberta, Edmonton, Alberta T6G 2H7, Canada*

**Peroxisomes are dynamic organelles that divide continuously in growing cell cultures and expand extensively in lipid-rich medium. Peroxisome population control is achieved in part by Pex11p-dependent regulation of peroxisome size and number. Although the production of Pex11p in yeast is tightly linked to peroxisome biogenesis by transcriptional regulation of the *PEX11* gene, it remains unclear if and how Pex11p activity could be modulated by rapid signaling. We report the reversible phosphorylation of *Saccharomyces cerevisiae* Pex11p in response to nutritional cues and delineate a mechanism for phosphorylation-dependent activation of Pex11p through the analysis of phosphomimicking mutants. Peroxisomal phenotypes in the *PEX11-A* and *PEX11-D* strains expressing constitutively dephosphorylated and phosphorylated forms of Pex11p resemble those of *PEX11* gene knock-out and overexpression mutants, although *PEX11* transcript and Pex11 protein levels remain unchanged. We demonstrate functional inequality and differences in subcellular localization of the Pex11p forms. Pex11Dp promotes peroxisome fragmentation when reexpressed in cells containing induced peroxisomes. Pex11p translocates between endoplasmic reticulum and peroxisomes in a phosphorylation-dependent manner, whereas Pex11Ap and Pex11Dp are impaired in trafficking and constitutively associated with mature and proliferating peroxisomes, respectively. Overexpression of cyclin-dependent kinase Pho85p results in hyperphosphorylation of Pex11p and peroxisome proliferation. This study provides the first evidence for control of peroxisome dynamics by phosphorylation-dependent regulation of a peroxin.**

Peroxisomes are a group of organelles characterized by high metabolic plasticity that act in a variety of important biochemical processes, notably the metabolism of lipids and the detoxification of reactive oxygen species. Although functional peroxisomes are essential for human survival, the conditional viability of yeast peroxisome biogenesis mutants has enabled the molecular identification of the core biogenic components of this organelle (1). Peroxisome biogenesis can be viewed as a complex developmental program that is initiated by the fatty acid-induced expression of many genes coding for peroxisomal proteins (2), followed by the stepwise assembly of the organelle. This highly regulated process can be divided into early and late events that are distinguished by the formation of pre-peroxisomal Pex3p-containing vesicles from the endoplasmic reticulum (ER)[2] (3, 4) and the entry of peroxisomal enzymes from the cytosol to form metabolically active peroxisomes. Different receptor-mediated import pathways for matrix (5) and membrane (6) proteins as well as a succession of distinct precursor populations (7) contribute to the orderly assembly of peroxisomes.

Peroxisome population control is accomplished by balancing peroxisome formation, division, and turnover and peroxisome partitioning to daughter cells (8). The Pex11 family of peroxisomal membrane proteins (PMPs) regulates peroxisome size and number in both higher and lower eukaryotes (for reviews, see Refs. 9 and 10). Pex11$\beta$-dependent peroxisome proliferation in mammals has been reported to be a multistep process involving the tubulation of peroxisomes, followed by constriction and scission of the elongated organelles into small, spherical units (11). Although Pex11 proteins are relatively abundant, their biochemical function remains obscure. Peroxisome division requires dynamin-related GTPases, because in their absence, peroxisomes are enlarged and sometimes have a "beads on a string" appearance (12). These observations support the view of an indirect rather than a direct role for Pex11p in the division process (*e.g.* by recruiting the fission machinery to peroxisomes or by promoting a modification of membrane curvature through its lipid binding activity) (13).

Peroxisomes divide constitutively in a growing cell culture but at the same time are able to proliferate extensively in response to the addition of lipids. The expression of the *PEX11* gene is tightly coupled to fatty acid-induced peroxisome proliferation with a range of promoter activation of more than 1000-fold between the repressed and induced states (14). Pex11p is below detection limits in cells growing exponentially in peroxisome-repressing medium and starts to accumulate slowly over several h when cells are transferred to growth in fatty acids. Deregulation of *PEX11* gene expression causes changes in cellular peroxisome abundance. Loss of Pex11p in yeast is linked to a reduction in the number of peroxisomes, together with an increase in the size and clustering of peroxisomes, whereas overexpression of the *PEX11* gene is associated with the hyperproliferation of peroxisomes (15, 16). In addition, Pex11p has been identified as an *in vitro* target of the nutrient- and cell

* This work was supported in part by Canadian Institutes of Health Research Grant 15131.

[S] The on-line version of this article (available at http://www.jbc.org) contains supplemental Figs. S1 and S2.

[1] International Research Scholar of the Howard Hughes Medical Institute. To whom correspondence should be addressed: Dept. of Cell Biology, University of Alberta, MSB 5-14, Edmonton, Alberta T6G 2H7, Canada. Tel.: 780-492-9868; Fax: 780-492-9278; E-mail: rick.rachubinski@ualberta.ca.

[2] The abbreviations used are: ER, endoplasmic reticulum; GFP, green fluorescent protein; mRFP, monomeric red fluorescent protein; MES, 4-morpholineethanesulfonic acid; PMP, peroxisomal membrane protein.

**TABLE 1**
***S. cerevisiae* strains used in this study**

| Strain | Genotype | Derivation |
|---|---|---|
| *BY4742* | *MATα, his3Δ1, leu2Δ0, lys2Δ0, ura3Δ0* | Ref. 43 |
| *pex11Δ* | *MATα, his3Δ1, leu2Δ0, lys2Δ0, ura3Δ0, pex11::KanMX4* | Ref. 43 |
| *pho85Δ* | *MATα, his3Δ1, leu2Δ0, lys2Δ0, ura3Δ0, pho85::KanMX4* | Ref. 43 |
| *Y262* | *MATa, ura3-52, his4-539, rpb1-1* | Ref. 23 |
| *PEX11-A* | *MATα, his3Δ1, leu2Δ0, lys2Δ0, ura3Δ0, pex11::PEX11 S165A, S167A* | This study |
| *PEX11-D* | *MATα, his3Δ1, leu2Δ0, lys2Δ0, ura3Δ0, pex11::PEX11 S165D, S167D* | This study |
| *POT1-GFP* | *MATα, his3Δ1, leu2Δ0, lys2Δ0, ura3Δ0, pot1::POT1-GFP (HIS5)* | This study |
| *pex11Δ/POT1-GFP* | *MATα, his3Δ1, leu2Δ0, lys2Δ0, ura3Δ0, pex11::KanMX4, pot1::POT1-GFP (HIS5)* | This study |
| *PEX11-A/POT1-GFP* | *MATα, his3Δ1, leu2Δ0, lys2Δ0, ura3Δ0, pex11::PEX11 S165A, S167A, pot1::POT1-GFP (HIS5)* | This study |
| *PEX11-D/POT1-GFP* | *MATα, his3Δ1, leu2Δ0, lys2Δ0, ura3Δ0, pex11::PEX11 S165D, S167D, pot1::POT1-GFP (HIS5)* | This study |
| *POT1-GFP/RTN1-mRFP* | *MATα, his3Δ1, leuΔ0, lys2Δ0, ura3Δ0, pot1::POT1-GFP (natR), rtn1::RTN1-mRFP (URA3)* | This study |
| *PEX11-A/POT1-GFP/RTN1-mRFP* | *MATα, his3Δ1, leu2Δ0, lys2Δ0, ura3Δ0, pex11::PEX11 S165A, S167A, pot1::POT1-GFP (natR), rtn1::RTN1-mRFP (URA3)* | This study |
| *PEX11-D/POT1-GFP/RTN1-mRFP* | *MATα, his3Δ1, leu2Δ0, lys2Δ0, ura3Δ0, pex11::PEX11 S165D, S167D, pot1::POT1-GFP (natR), rtn1::RTN1-mRFP (URA3)* | This study |
| *GAL1PEX11/POT1-GFP* | *MATα, his3Δ1, leu2Δ0, lys2Δ0, ura3Δ0, pex11::GAL1PEX11 (KanMX4), pot1::POT1-GFP (HIS5)* | This study |
| *GAL1PEX11-D/POT1-GFP* | *MATα, his3Δ1, leu2Δ0, lys2Δ0, ura3Δ0, pex11-d::GAL1PEX11-D (KanMX4), pot1::POT1-GFP (HIS5)* | This study |

cycle-dependent yeast kinases, Rim15p and Pho85p (17), whereas Pex11$\beta$ has been shown to be phosphorylated in a human cell line (18). We therefore sought to determine whether modification by phosphorylation could provide an additional mechanism for regulation of Pex11p in yeast.

Here we show that Pex11p is phosphorylated at $Ser^{165}$ and/or $Ser^{167}$ in yeast. The analysis of mutant forms of Pex11p locked into states of constitutive dephosphorylation or phosphorylation demonstrates that phospho-Pex11p is active in promoting peroxisome proliferation. Wild-type Pex11p translocates between ER and peroxisomes in response to changes in its phosphorylation state, which can be either nutrient-induced or elicited by overexpression of Pho85p kinase. The dephosphorylated and phosphorylated mutant forms of Pex11p, on the other hand, are permanently associated with either mature peroxisomes or hyperproliferating peroxisomes at an ER-peroxisome interface. Our work provides evidence for regulation of organelle dynamics by phosphorylation-controlled protein trafficking and furthermore demonstrates that Pex11p-dependent peroxisome population control is accomplished by the combined effect of *PEX11* gene regulation and posttranslational modification of Pex11p activity.

## EXPERIMENTAL PROCEDURES

*Yeast Strains, Culture, and Genetic Manipulation—Saccharomyces cerevisiae* strains used in this study are listed in Table 1. Unless stated otherwise, all strains were cultured at 30 °C. Media used were as follows: YPD, 1% yeast extract, 2% peptone, 2% glucose; YPBO, 0.3% yeast extract, 0.5% peptone, 0.5% potassium phosphate buffer, pH 6.0, 0.2% Tween 40, 1% oleic acid; SCIM, 0.5% yeast extract, 0.5% peptone, 0.67% yeast nitrogen base without amino acids, 0.5% Tween 40, 0.3% glucose, 0.3% oleic acid, 1× Complete Supplement Mixture (Bio 101, Inc., Vista, CA); CSM − ura, 0.67% yeast nitrogen base without amino acids, 2% glucose, 1× Complete Supplement Mixture − ura; SCIM − ura, 0.67% yeast nitrogen base without amino acids, 0.5% Tween 40, 0.3% glucose, 0.3% oleic acid, 1× Complete Supplement Mixture − ura. To construct strains expressing the peroxisomal reporter Pot1p-GFP, sequence coding for *Aequoria victoria* GFP was inserted chromosomally in frame at the 3′-end of the *POT1* gene encoding Pot1p (peroxisomal 3-ketoacyl-CoA thiolase). For construction of strains expressing the cortical ER reporter Rtn1p-mRFP, sequence coding for monomeric red fluorescent protein (mRFP) from *Discosoma* sp. was inserted chromosomally in frame at the 3′-end of the *RTN1* gene. To construct strains for galactose-inducible *PEX11* gene expression, the *GAL1* promoter was introduced immediately upstream of the *PEX11* ORF by PCR-based integrative transformation of yeast cells. The *delitto perfetto* strategy (19) was used to modify the *PEX11* genomic locus without introduction of *ex situ* sequence. Site-directed mutagenesis of the region coding for the Pex11p phosphorylation motif was done by PCR-based amplification of cassettes comprising the *PEX11* ORF using the oligonucleotides 5′-CAAGGCAAAAGCACAAGCCCAAGGCGATG (A mutations) and 5′-GTCAAGGCAAAAGACCAAGACCAAGGCGATG (D mutations) and subsequent replacement of a CORE element inserted in the *PEX11* locus with the mutagenic cassettes (19). Genomic integrations were confirmed by PCR, whereas *delitto perfetto*-based modifications of genomic regions were also verified by sequencing the entire *PEX11* ORF and 500 bp in both the 5′- and 3′-flanking regions.

*Confocal Fluorescence Microscopy and Immunofluorescence Microscopy*—Live cell confocal microscopy was performed essentially as described (20). To visualize Pot1p-GFP fluorescence, images were acquired as *z*-stacks at 125-nm intervals using a modified LSM510 META confocal microscope equipped with a Plan-Apochromat ×63/1.4 numerical aperture oil differential interference contrast objective (Carl Zeiss) with the microscope pinhole adjusted to 1 Airy unit. A piezoelectric actuator was used to drive continuous objective movement, allowing for the rapid collection of *z*-stacks. GFP was excited with a 488-nm laser, and its emission was collected using a 505-nm long pass filter. Acquired three-dimensional data sets of the GFP fluorescence channel were deconvolved using algorithms provided by Huygens Professional Software (Scientific Volume Imaging). Images were processed to remove noise and reassign blur through an iterative classic maximum likelihood estimation algorithm and a theoretical point spread function. The transmission image was treated differently. Blue color was applied to the transmission image using Imaris software (version 6.1, Bitplane). The level of the transmission image was modified, and the image was processed until only the circum-

ference of the cell was visible. Interference from internal structures captured in the transmission images was removed in Photoshop (Adobe). Imaris was used to display the deconvolved three-dimensional data set of the GFP channel with the processed transmission image before final figure assembly in Photoshop. Peroxisome numbers per cell were manually counted in at least 150 randomly captured cells per strain and time point using the spot counting tool of the Imaris imaging software.

To image the intracellular distribution of Pex11p relative to ER and peroxisome markers by immunofluorescence microscopy, cells were fixed by the addition of 0.1 volume of 37% formaldehyde to the medium and then spheroblasted. Pex11p was labeled with affinity-purified anti-Pex11p antibodies and Cy5-conjugated secondary antibodies (Jackson ImmunoResearch). Images were acquired as *z*-stacks at 300-nm intervals on a Zeiss Imager.Z1 epifluorescence microscope using a Plan-Apochromat ×100/1.4 numerical aperture oil differential interference contrast objective and 470/40, 546/12, and 640/30 band pass filters for excitation and 525/50, 575–640, and 690/50 band pass filters for emission of the GFP, red fluorescent protein, and Cy5 fluorescence channels, respectively. Three-dimensional data sets of the fluorescence channels were deconvolved as described above and displayed as maximum intensity projections using Imaris software prior to final image assembly in Photoshop.

*Transmission Electron Microscopy*—Fixation and processing of cells for transmission electron microscopy were carried out as described (21). Morphometric analysis was performed using algorithms developed by Weibel and Bolender (22).

*Analysis of Transcript and Protein Abundance*—Total RNA was extracted from yeast cells by hot acidic phenol. Contaminating chromosomal DNA was removed by treatment with DNase I. 20 $\mu$g of RNA was separated in 1.25% agarose gels containing 6% formaldehyde. RNA was blotted onto nylon membranes in 20× SSC and cross-linked to the membrane by transillumination. Blots were hybridized under stringent conditions in Rapid Hyb buffer (Amersham Biosciences) with gene-specific probes that were $^{32}$P-labeled using the Prime-It II random primer labeling kit (Stratagene). Blots were washed in 50% formamide and subjected to autoradiography.

For the transcriptional shut-off assay, *S. cerevisiae* strain *Y262* carrying a temperature-sensitive RNA polymerase II gene (23) was cultured for 15 h in SCIM at 25 °C to induce expression of the *PEX11* gene. The culture was divided equally and resuspended in either YPBO or YPD medium. After 30 min of recovery at 25 °C, each culture was abruptly shifted to 39 °C by the addition of an equal volume of medium prewarmed to 50 °C. Equal aliquots of culture were removed at regular intervals after the temperature shift, and cells were rapidly harvested and frozen in liquid nitrogen. RNA extraction and Northern blotting were performed as described above. Transcripts were quantified using a Storm 840 PhosphorImager, and a nonlinear least squares model was applied to determine the half-life of the mRNA.

Whole cell lysates were prepared as described (24) and analyzed by SDS-PAGE and immunoblotting using horseradish peroxidase-conjugated secondary antibodies and the ECL detection system (Amersham Biosciences). Pex11p-specific antisera were raised in guinea pig (anti-Pex11p Q8) and rabbit (anti-Pex11p P85) against the peptide GDEHEDHKKVLGK, comprising aminoacyl residues 169–181 of Pex11p, and affinity-purified on immobilized peptide. Anti-Pex11p antiserum Q23 was raised in rabbit against an N-terminal fragment of Pex11p comprising amino acids 1–133 and affinity-purified on recombinant protein. Affinity-purified antibodies were used at a concentration of 0.25 $\mu$g/ml for immunoblotting and at a 10-fold higher concentration for immunofluorescence microscopy. All antibodies were characterized for their ability to bind native and denatured Pex11p. Antibodies Q8 and P85 recognize both native and denatured Pex11p, whereas antibody Q23 recognizes only denatured Pex11p. Only antibody Q8 was found to immunoprecipitate Pex11p from enriched peroxisomal fractions. Pot1p-, Pex3p-, and actin-specific antibodies have been described (4, 24, 25).

The stability of Pex11p was determined in cycloheximide chase assays as described (26). To block protein synthesis, cell cultures were treated with cycloheximide at a final concentration of 50 $\mu$g/ml and sampled periodically for immunoblot analysis. Immunoblots were quantified using a GS-800 densitometer and Quantity One version 4.3.1 software (Bio-Rad).

*Metabolic Labeling and Subcellular Fractionation*—Peroxisomes were isolated from cells after *in vivo* labeling with [$^{32}$P]orthophosphate essentially as described (27). Specifically, 5 $A_{600}$ units of cells growing exponentially in YPD were seeded into 100 ml of SCIM and grown for 15 h. Cells were either metabolically labeled during growth in SCIM with 10 $\mu$Ci/ml $H_3{}^{32}PO_4$ and directly harvested, or cells were first grown in nonradioactive SCIM, pelleted, and resuspended in the same volume of YPD for 2 h and metabolically labeled during that time. Cells were harvested, washed with water, and spheroblasted with 2 mg of zymolyase 100T/g of cells for 45 min at 30 °C. Spheroblasts were disrupted by homogenization in buffer H (0.6 M sorbitol, 2.5 mM MES, pH 5.5, 1 mM KCl, 1 mM EDTA, 1× complete protease inhibitors (Roche Applied Science), 1× phosphatase inhibitor mixture (AG Scientific)). Cell debris and nuclei were pelleted from the homogenate by five successive centrifugations at 1,000 × *g* for 6 min each to generate a postnuclear supernatant, which was subsequently subjected to centrifugation at 20,000 × *g* for 35 min to yield supernatant and pellet fractions. The pellet fraction was resuspended in buffer H containing 11% Nycodenz and 1× complete protease inhibitors and overlaid onto a discontinuous gradient consisting of 17, 25, 35, and 50% Nycodenz in buffer H containing complete protease inhibitors. Organelles were separated by centrifugation at 100,000 × *g* for 65 min in a Beckman NVT65.2 rotor. 275-$\mu$l fractions were collected from the bottom of the gradient.

For metabolic labeling of cells harboring either a control plasmid or a *PHO85* gene overexpression plasmid (pBY011 (28) and pBY011-PHO85, respectively), 10 $A_{600}$ units of cells growing exponentially in CSM − ura were seeded into 100 ml of SCIM − ura and grown for 15 h in the presence of 10 $\mu$Ci of $H_3{}^{32}PO_4$/ml. Peroxisomes were isolated as described above.

*Immunoprecipitation of Pex11p*—Peak peroxisome fractions obtained by discontinuous density gradient centrifugation were used for immunoprecipitation of Pex11p. Organelles present in

these fractions were diluted 5-fold in buffer H, pelleted by centrifugation at 245,000 × *g* in a TLA120.2 rotor at 4 °C for 45 min, and resuspended in 100 μl of denaturing extraction buffer (50 mM Tris-HCl, pH 7.4, 1% SDS, 1× complete protease inhibitors). After boiling for 10 min, the protein extracts were diluted by the addition of 900 μl of 50 mM Tris-HCl, pH 7.4, 2% bovine serum albumin, and incubated on ice for 10 min. Pex11p was recovered by immunoprecipitation for 2 h on ice using 2 μg of an IgG fraction of antibody Q8 and adsorbed onto fixed *Staphylococcus aureus* cells (Calbiochem). Immunoprecipitates were washed four times in 50 mM Tris-HCl, pH 7.4, separated by SDS-PAGE, and analyzed by either autoradiography or immunoblotting with antibodies P85 and Q23.

## RESULTS

*Pex11p Is a Phosphoprotein*—Computational analysis predicted a high probability of phosphorylation of Pex11p at $Ser^{165}$ and $Ser^{167}$ (Fig. 1*A*). Phosphomimicking mutants of Pex11p were constructed by genomic replacement of sequences in the *PEX11* gene encoding both serines with triplets coding for alanine or aspartic acid using the *delitto perfetto* transformation strategy, which enables the modification of yeast genomic regions without leaving traceable *ex situ* changes (19). The strains obtained were designated *PEX11-A* and *PEX11-D*. To determine whether Pex11p is phosphorylated in live cells at the predicted residues, we measured its incorporation of [$^{32}$P]orthophosphate under different environmental conditions. Peroxisome formation and Pex11p synthesis were initiated by culturing cells for 15 h in oleate-containing medium (SCIM) that enables both cell growth and peroxisome proliferation. Subcellular fractions enriched for peroxisomes were isolated from cultures that had been labeled metabolically *in vivo* with [$^{32}$P]-orthophosphate either during growth in SCIM or after transfer for 2 h to rich medium (YPD) (Fig. 1*B*), and the presence of Pex11p in the peroxisomal fractions was confirmed by immunoblotting (Fig. 1*C*). Pex11p was recovered from these fractions by immunoprecipitation. The $^{32}$P-labeled form of Pex11p could be detected in autoradiograms of immunoprecipitates from wild-type cells but not from *pex11*Δ or *PEX11-D* cells (Fig. 1*D*). Total Pex11p in the immunoprecipitates was present at similar concentrations in samples from wild-type and *PEX11-D* cells and absent in samples from *pex11*Δ cells (Fig. 1*E*). Quantitative comparison between phosphorylated (Fig. 1*D*) and total (Fig. 1*E*) Pex11p revealed a more than 3-fold increase in phosphorylated Pex11p in YPD- *versus* SCIM-grown cells (Fig. 1*F*). These data led us to conclude that Pex11p is phosphorylated in wild-type yeast cells at $Ser^{165}$ and/or $Ser^{167}$ and that its phosphorylation state is dependent on nutritional cues.

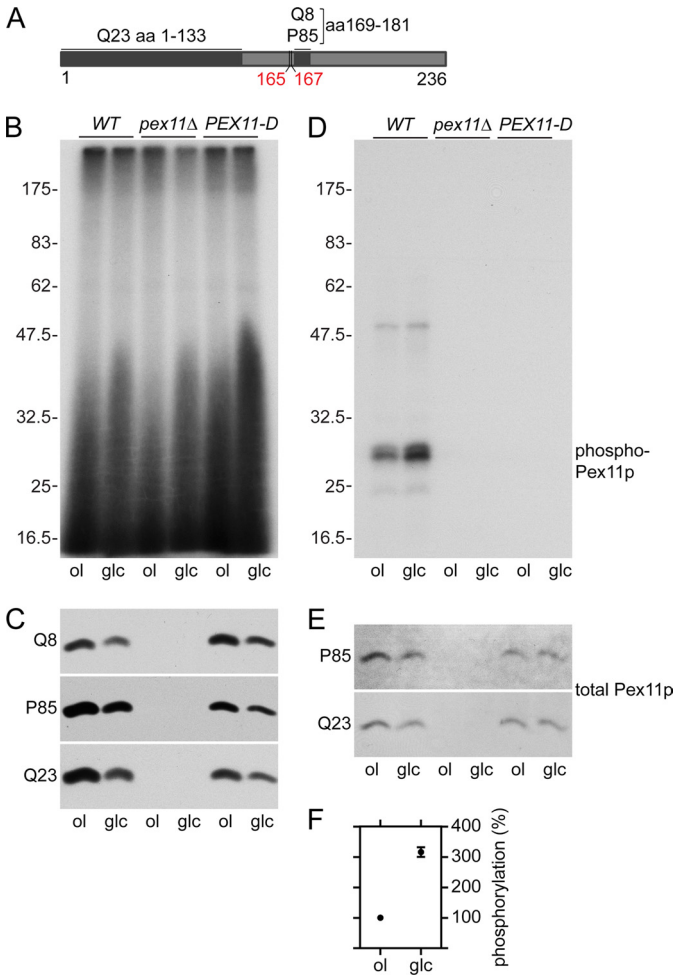


FIGURE 1. ***In vivo* phosphorylation of Pex11p.** *A*, phosphorylation of Pex11p at $Ser^{165}$ and $Ser^{167}$ (*red*) was predicted by the NetPhos 2.0 server (available on the World Wide Web). The binding regions for anti-Pex11p antibodies Q23, Q8, and P85 are shown in *dark gray*. See "Experimental Procedures" for antibody details. *B*, 5 μg of total peroxisomal fractions obtained by discontinuous density gradient centrifugation from wild-type (*WT*), *pex11*Δ, and *PEX11-D* cells were separated by SDS-PAGE and subjected to autoradiography. Before fractionation, cells were grown either for 15 h in oleate-containing SCIM containing 10 μCi $H_3PO_4$/ml (*ol*) or for 15 h in SCIM and then in glucose-containing YPD containing 10 μCi $H_3PO_4$/ml for 2 h (*glc*). *C*, total peroxisome fractions as shown in *B* were probed for the presence of Pex11p by immunoblotting with antibodies Q8, P85, and Q23. *D*, $^{32}$P-labeled Pex11p was immunoprecipitated from the peroxisome fractions in *B* with antibody Q8, separated by SDS-PAGE, and detected by autoradiography. *Numbers* on the *left* in *B* and *D* represent the migrations of molecular mass markers in kDa. *E*, the immunoprecipitates in *D* were probed for total Pex11p by immunoblotting with antibodies P85 and Q23. *F*, densitometric analysis of bands presented in *D* and *E* was used to determine the ratios of phosphorylated Pex11p to total Pex11p. Phosphorylation of Pex11p in YPD-grown cells is plotted relative to the phosphorylation of Pex11p in SCIM-grown cells, which was normalized to 100%. The *symbols* present the means of three independent experiments. *Bars*, S.E. *aa*, amino acids.

*Pex11p Phosphomimicking Mutants Resemble PEX11 Gene Overexpression and Knock-out Phenotypes*—We examined the implications of artificially locking Pex11p in a state of constitutive phosphorylation or constitutive dephosphorylation on the process of peroxisome formation. To this end, we initiated peroxisome biogenesis by growing wild-type and *PEX11* mutant cells harboring the peroxisomal marker Pot1p-GFP in peroxisome-repressing, glucose-containing YPD medium and then resuspending them in peroxisome-inducing, oleate-containing YPBO medium. Peroxisome formation was observed by confocal fluorescence microscopy over a period of 20 h. Peroxisomes became visible within 2 h after transfer, and peroxisome morphologies in the wild-type and *PEX11* mutant cells became divergent with continued incubation in YPBO. Distinct peroxisomal phenotypes were apparent in wild-type and mutant cells by 6–8 h (Fig. 2). Peroxisomes appeared enlarged and clustered in the *pex11*Δ and *PEX11-A* mutants, whereas they were small, elongated, and hyperproliferated in the *PEX11-D* mutant. Per-

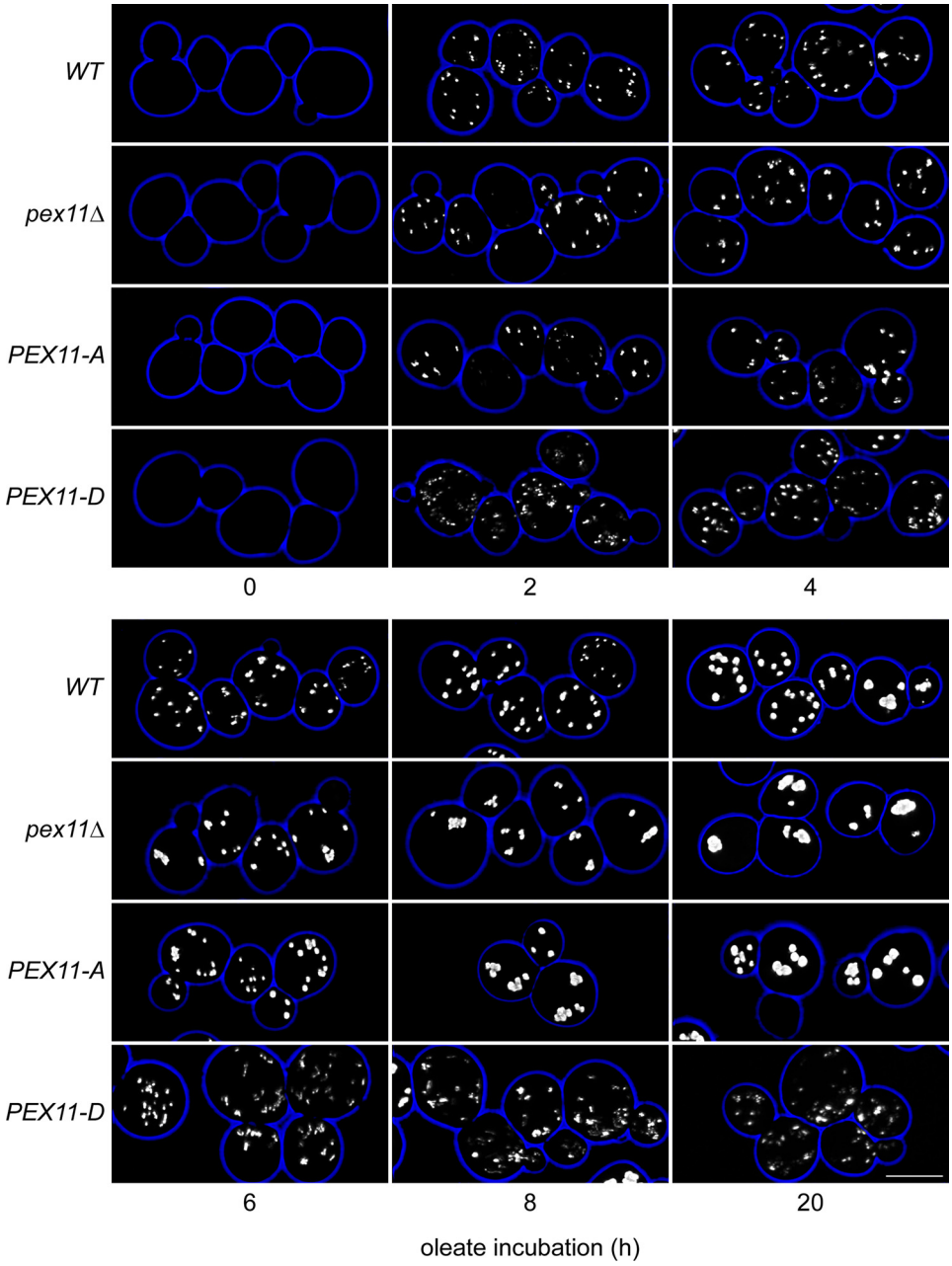


FIGURE 2. **Time course of peroxisome formation in wild-type and Pex11p phosphomimicking mutant cells.** Wild-type and isogenic *PEX11* mutant cells expressing genomically encoded Pot1p-GFP as a fluorescent peroxisome reporter were cultured to late exponential phase in glucose-containing YPD medium, collected by centrifugation, and resuspended in the same volume of oleate-containing YPBO medium. Peroxisome formation was visualized by confocal fluorescence microscopy over a period of 20 h. GFP fluorescence images were acquired as *z*-stacks and deconvolved and are presented as maximum intensity projections. *Bar*, 5 $\mu$m.

oxisomes were also examined by transmission electron microscopy. Peroxisomes were typically found as single entities in the cortical regions of wild-type and *PEX11-D* cells, whereas *pex11*Δ and *PEX11-A* cells frequently contained clustered peroxisomes (Fig. 3). Morphometric analysis confirmed an increase in peroxisome size and clustering in the *pex11*Δ mutant, as well as a decrease in peroxisome size concomitant with an increase in peroxisome numbers in the *PEX11-D* mutant (Table 2). Although peroxisomes in the *PEX11-A* mutant were not significantly different in size from peroxisomes in the wild-type strain, the extensive clustering observed in the *PEX11-A* mutant may contribute to the appearance of fewer and enlarged peroxisomes in light microscopy (Fig. 2 and Table 2).

In summary, the observed hypo- and hyperproliferation of peroxisomes in *PEX11-A* and *PEX11-D* cells are strongly reminiscent of the phenotypes previously described for *PEX11* gene deletion and overexpression strains, respectively (15, 16).

*PEX11 Transcript and Pex11 Protein Levels Are Unaltered in the Phosphomimicking Mutants*—Relative transcript and protein abundance of various peroxisomal markers with time of oleate incubation was determined to ascertain whether the phenotypes observed in the phosphomimicking mutants were due to changes in *PEX11* gene expression and/or Pex11 protein levels. *PEX11* and *POT1* genes share a similar promoter structure and are strongly inducible by fatty acids (14, 29), whereas *PEX3* expression is only weakly responsive to the presence of fatty acids (27) and can therefore be used for normalization of data. When cells were transferred from glucose-containing YPD medium to oleate-containing YPBO medium, robust up-regulation of *PEX11* transcript over time was observed (Fig. 4*A*). *PEX11* transcript abundance was similar in wild-type and mutant strains.

Immunoblot analyses using different Pex11p-specific antibodies revealed differences in their ability to recognize the constitutively dephosphorylated and constitutively phosphorylated forms of Pex11p (Fig. 4*B*). Using antibody Q8, we observed decreased levels of Pex11Ap and increased levels of Pex11Dp. Although Pex11p became detectable in wild-type cells at 2 h of oleate incubation and continued to accumulate over time, Pex11Ap was greatly reduced in overall amount and only became detectable at 8 h of incubation in oleate medium. In contrast, Pex11Dp was already detectable in glucose-grown cells (0 h) and accumulated massively with time after transfer to oleate medium (Fig. 4*B*). Conversely, immunoblotting with antibody P85 showed that Pex11p accumulated with similar kinetics and abundance in the wild-type and phosphomimicking strains after transfer to oleate medium (Fig. 4*B*). Similar results were obtained when probing with antibody Q23 or with an anti-GFP antibody to

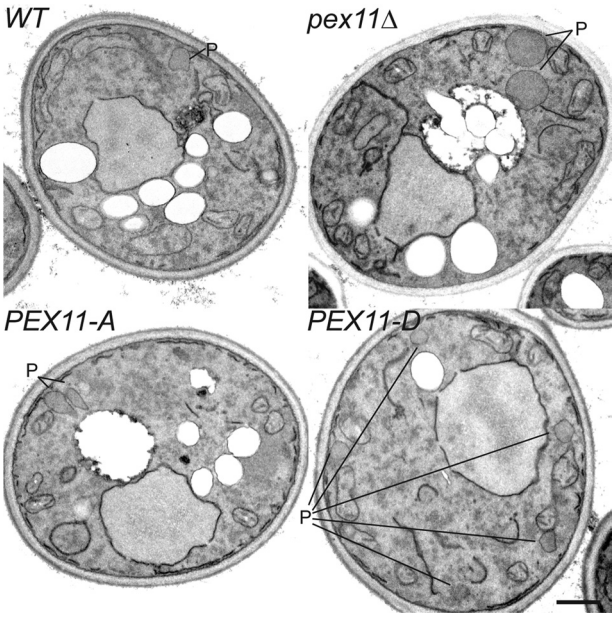


FIGURE 3. **Peroxisome ultrastructure in wild-type and Pex11p phosphomimicking mutant cells.** The same strains as in Fig. 2 were grown for 16 h in oleate-containing SCIM and processed for electron microscopy. *WT*, wild type. *P*, individual peroxisomes. *Bar*, 0.5 μm.

**TABLE 2**

**Morphometric analysis of peroxisomes**

Values were determined from three independent experiments in which over 200 micrographs per strain were analyzed.

| Strain | Average peroxisome area ± S.E | Numerical density of peroxisomes[a] | Clustered peroxisomes[b] |
|---|---|---|---|
| | $\mu m^2$ | *peroxisomes/*$\mu m^3$ | *% of total* |
| Wild type | 0.035 ± 0.0011 | 1.14 | 8.75 |
| *pex11*Δ | 0.079 ± 0.0032[c] | 0.65 | 20.85 |
| PEX11-A | 0.039 ± 0.0013 | 1.21 | 18.52 |
| PEX11-D | 0.017 ± 0.00076[c] | 4.46 | 7.86 |

[a] Density is shown in number of peroxisomes/$\mu m^3$ of cell volume (22).
[b] A peroxisome was designated as "clustered" if it was less than its own diameter apart from a neighboring peroxisome.
[c] Significantly different from the measurement of the wild-type strain as determined by a non-parametric Kruskal-Wallis test ($p < 0.0001$), followed by Dunn's multiple comparison test ($p < 0.05$).

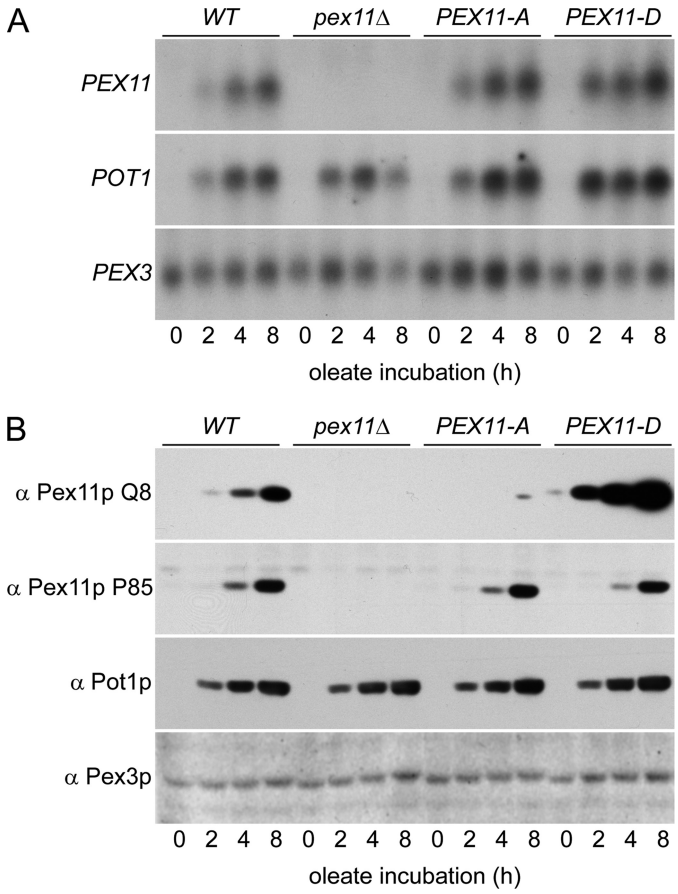


FIGURE 4. ***PEX11* transcript and Pex11 protein levels in phosphomimicking mutants.** *A*, Northern blots of total RNA prepared from wild-type (*WT*) and *PEX11* mutant strains. Cells were grown to late exponential phase in glucose-containing YPD medium and then resuspended in the same volume of oleate-containing YPBO medium. Samples were withdrawn at 0, 2, 4, and 8 h of incubation in YPBO. Blots were hybridized with probes specific for the *PEX11*, *POT1*, and *PEX3* genes. *B*, immunoblots of whole cell lysates prepared from the same cultures as in *A* probed with the Pex11p-specific antibodies Q8 and P85 as well as with Pot1p- and Pex3p-specific antibodies. One of four independent experiments with similar results is presented.

detect genomically encoded Pex11p-GFP fusion proteins (data not shown). Thus, antibody Q8 cannot faithfully detect overall cellular Pex11p, perhaps because the epitope to which it was raised is near the sites of Pex11p phosphorylation (Fig. 1*A*), and dynamic changes at these sites resulting from phosphorylation and dephosphorylation could affect recognition of Pex11 protein by antibody Q8.

*Phosphomimetic Pex11Dp Actively Promotes Peroxisome Proliferation*—To elucidate whether the phosphorylated and dephosphorylated forms of Pex11p are intrinsically different in their activities, we measured the effect of their reintroduction into cells with preformed peroxisomes. We inserted the inducible *GAL1* promoter upstream of the *PEX11*, *PEX11-A*, and *PEX11-D* genes to dissociate their expression from induction by oleate and then initiated their expression by the addition of galactose. Peroxisome formation was begun by culturing these strains containing the peroxisomal reporter Pot1p-GFP for 15 h in oleate-containing SCIM. At the time of galactose addition, Pex11 proteins were not detectable (Fig. 5*A*), and the typical *pex11*Δ phenotype of a few enlarged and clustered peroxisomes was apparent (Fig. 5*B*). Expression of the different *PEX11* genes following galactose addition was monitored by immunoblotting for the wild-type and mutant forms of Pex11p (Fig. 5*A*). Pex11Ap was not produced at detectable levels under these conditions in several independent transformants carrying *GAL1* promoter insertions or even in a strain carrying an additional high copy number galactose-inducible plasmid. Therefore, Pex11Ap was excluded from further analysis. In contrast, Pex11p and Pex11Dp were expressed at comparable levels, as determined by immunoblotting with antibody P85 (Fig. 5*A*). Peroxisomes started to divide 30 min following galactose addition, and elongation of peroxisomes was observed in cells of the *PEX11-D* strain at this time (Fig. 5*B*). By 120 min of galactose addition, dramatic differences in peroxisome morphology and numbers were apparent in cells of the wild-type and *PEX11-D* strains. Cells expressing Pex11p typically contained 25 or fewer peroxisomes, and only a few elongated peroxisomes per cell were observed (Fig. 5, *B* and *C*). In contrast, cells expressing Pex11Dp contained peroxisomes that were irregularly shaped and elongated and, in a significant proportion of cells, between 25 and 100 peroxisomes were present (Fig. 5, *B* and *C*). We

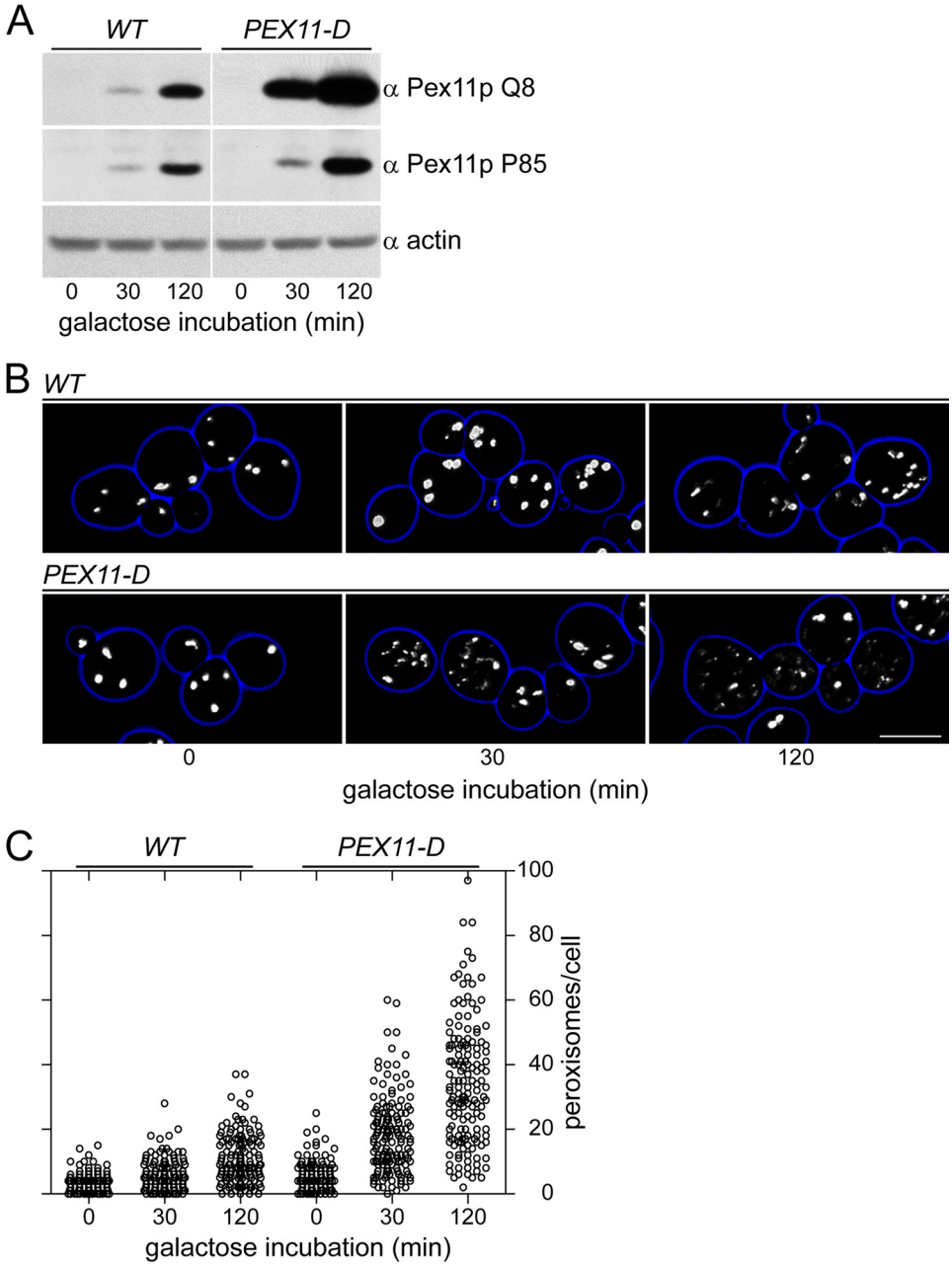


FIGURE 5. **Pex11Dp actively promotes peroxisome proliferation.** *A*, comparison of Pex11p and Pex11Dp production arising from transcription of their respective genes under control of the *GAL1* promoter. Wild-type (*WT*) and *PEX11-D* mutant cells containing an integrated *GAL1* promoter upstream of the *PEX11* and *PEX11-D* genes and harboring the Pot1p-GFP peroxisomal marker were cultured for 15 h in oleate-containing SCIM to induce peroxisome formation. Expression of Pex11p and Pex11Dp was then induced by the addition of galactose to a final concentration of 0.5%. Samples were withdrawn at 0, 30, and 120 min after galactose addition. Immunoblots of total cell lysates were performed with antibodies Q8 and P85 and antibodies to actin, which served as a loading control. *B*, peroxisome phenotypes in cells reexpressing Pex11p and Pex11Dp after galactose addition. Fluorescence images of the GFP channel at 0, 30, and 120 min after galactose addition to the same cells as in *A* were recorded as *z*-stacks and deconvolved and are presented as maximum intensity projections. *Bar*, 5 $\mu$m. *C*, peroxisome numbers per cell in the wild-type and *PEX11-D* strains at 0, 30, and 120 min after galactose addition. Peroxisome counts were performed on 50 randomly recorded cells per time point and strain. All peroxisome counts from three independent experiments are shown.

observed hyperproliferation of peroxisomes in the *PEX11-D* strain even when reducing the concentration of Pex11Dp significantly below the concentration of Pex11p through titration of the amount of galactose added (data not shown). Furthermore, continued galactose-driven expression of Pex11Dp frequently led to a complete fragmentation of existing peroxisomes and a concomitant loss of Pot1p-GFP signal (data not shown). Our findings show that Pex11Dp actively promotes peroxisome division and suggest that phosphorylation of Pex11p leads to its activation in its role in the peroxisome proliferation process.

*Pex11p Localization to the Endoplasmic Reticulum and Peroxisomes Is Altered in the Pex11p Phosphomimicking Mutants*—To begin to understand how phosphorylation might act on Pex11p in the cell, we examined its intracellular distribution under conditions leading to changes in its phosphorylation state. Pex11 proteins have previously been reported to be confined to the peroxisomal membrane (for reviews, see Refs. 9, 10, and 30). However, we observed by immunofluorescence microscopy that the exclusively punctate pattern of a typical peroxisomal protein could not always be established for Pex11p. We assessed the localization of Pex11p relative to markers for cortical ER and peroxisomes (Fig. 6, *WT*). Detection with antibody Q8 showed Pex11p in patch-like elements at the cell periphery of SCIM-grown wild-type cells. Remarkably, Pex11p and Pot1p did not colocalize extensively but compartmentalized to different structures. A high degree of overlap of Pex11p with the cortical ER protein Rtn1p suggested an ER localization of Pex11p under these conditions (Fig. 6*A*, *WT*). The affinity of antibody Q8 for Pex11Dp (see Fig. 4*B*) could lead to a preferential recognition of the phosphorylated form(s) of Pex11p in immunofluorescence microscopy. Comparison with the staining pattern obtained with the Pex11p concentration-dependent antibody P85 revealed a broader distribution of Pex11p and cocompartmentalization with both Rtn1p and Pot1p (Fig. 6*A*, *WT*). Transfer of cells to glucose-containing YPD medium, previously shown to increase the phosphorylation of Pex11p (see Fig. 1*D*), elicited extensive changes in the intracellular distribution of Pex11p. Within 2 h after transfer to YPD medium, both the Q8 and P85 antibodies detected the entire Pex11p pool no longer in the cortical ER but colocalizing with Pot1p-positive structures

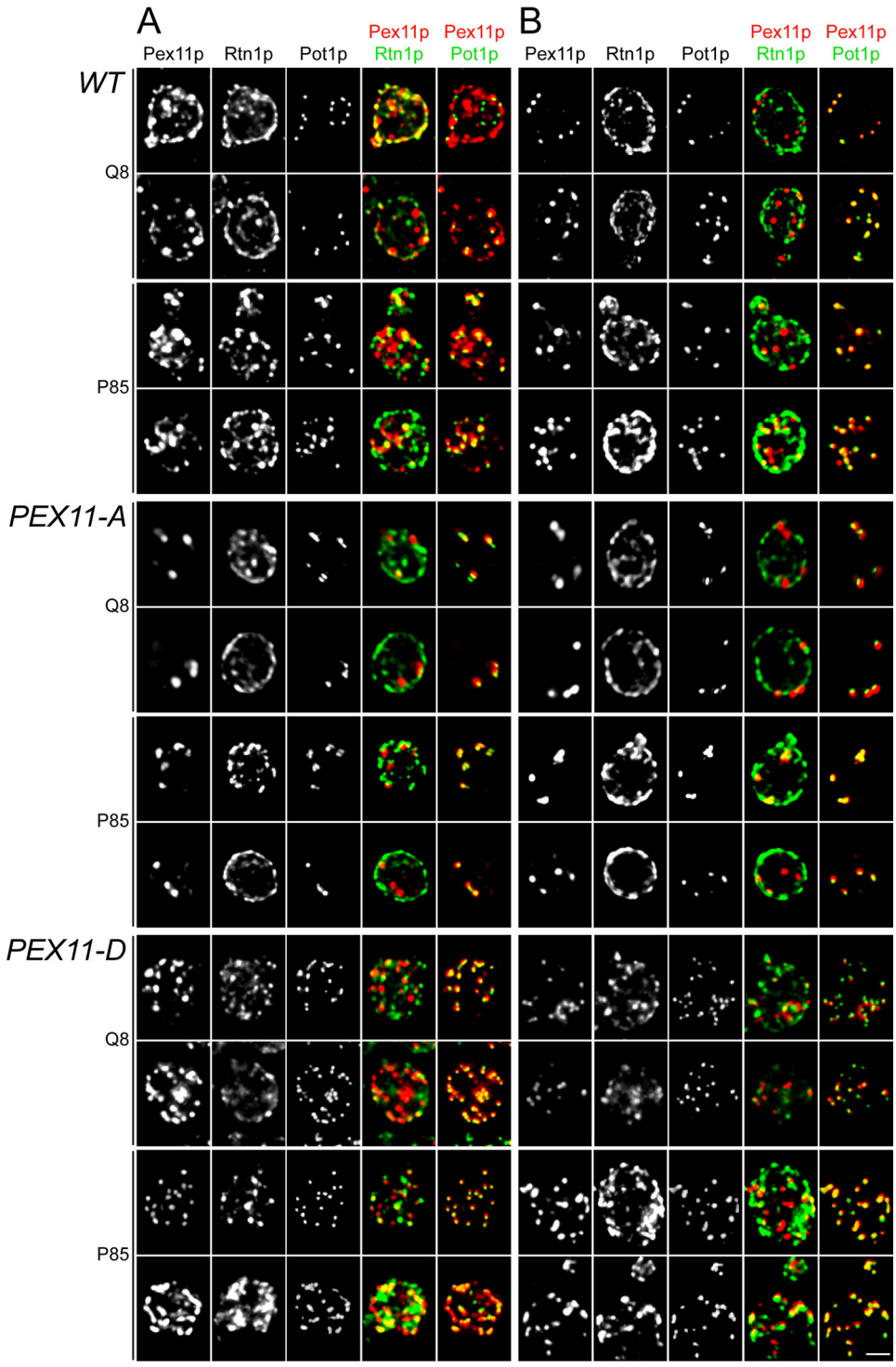


FIGURE 6. **Nutrient-dependent changes in the compartmentalization of Pex11p.** Immunofluorescence microscopy of Pex11p localization in wild-type (*WT*) and *PEX11* mutant strains. Cells harboring the markers Rtn1p-mRFP and Pot1p-GFP for cortical ER and peroxisomes, respectively, were cultured for 15 h in SCIM and fixed directly (*A*), or a fraction of them was transferred to YPD medium and incubated for 2 h prior to fixation (*B*). Pex11p was detected by anti-Pex11p antibodies Q8 and P85 and Cy5-conjugated secondary antibodies. GFP, mRFP, and Cy5 fluorescence images were acquired as *z*-stacks and deconvolved and are presented as maximum intensity projections. Single channel presentations are in monochrome mode. In the *merged images*, Pex11p- and Rtn1p/Pot1p-specific signals are *pseudocolored red* and *green*, respectively. No Pex11p-specific signal was detectable in the *pex11*Δ mutant by either Q8 or P85 antibody, and organelle morphologies in all strains were the same when Pex11p was not immunodecorated (data not shown). *Bar*, 2 μm.

from wild-type Pex11p (Fig. 6, *A* and *B*). In both SCIM and YPD medium, Pex11Ap was confined to a few punctae that closely followed the distribution of Pot1p and did not overlap with Rtn1p. Pex11Dp was found in punctate and reticular elements in close apposition to numerous Pot1p-positive and Rtn1p-positive foci and therefore appeared to be enriched at a potential ER-peroxisome interface. Importantly, there were no differences in detection of Pex11Ap and Pex11Dp by antibodies Q8 and P85, and no changes in the intracellular distribution of Pex11Ap and Pex11Dp were observed after shifting cells from SCIM to YPD medium (Fig. 6, *A* and *B*). Therefore, the change in intracellular distribution upon the shift from oleate-containing SCIM to glucose-containing YPD appears to be a feature of wild-type Pex11p alone. We also noticed that the different compartmentalization of Pex11p, Pex11Ap, and Pex11Dp affected not only peroxisome abundance but also the organization of the cortical ER. Irrespective of nutrient condition, cortical ER was ring-shaped and peripherally located in cells of the *PEX11-A* mutant, whereas it was highly fragmented and distributed generally in cells of the *PEX11-D* mutant. In wild-type cells, the cortical ER structure usually became less fragmented and more continuous after the shift from SCIM to YPD medium.

The observed differences in the intracellular localization of wild-type Pex11p could be due to either the trafficking of preexisting Pex11p from the ER to peroxisomes or to the import by peroxisomes of newly synthesized Pex11p followed by its degradation at the ER. To distinguish between these possibilities, we used transcriptional and translational shut-off assays to examine the effect of incubating cells in oleate (YPBO) or glucose (YPD) medium on the stability of *PEX11* transcript and Pex11 protein. We found that *PEX11* transcript was rapidly destabilized in YPD, whereas Pex11 protein was stable in both YPBO and YPD (supplemental Fig. S1). Because Pex11p cannot

(Fig. 6*B*, *WT*). Pex11Ap mimicking constitutively dephosphorylated Pex11p and Pex11Dp mimicking constitutively phosphorylated Pex11p differed strongly in their patterns of localization

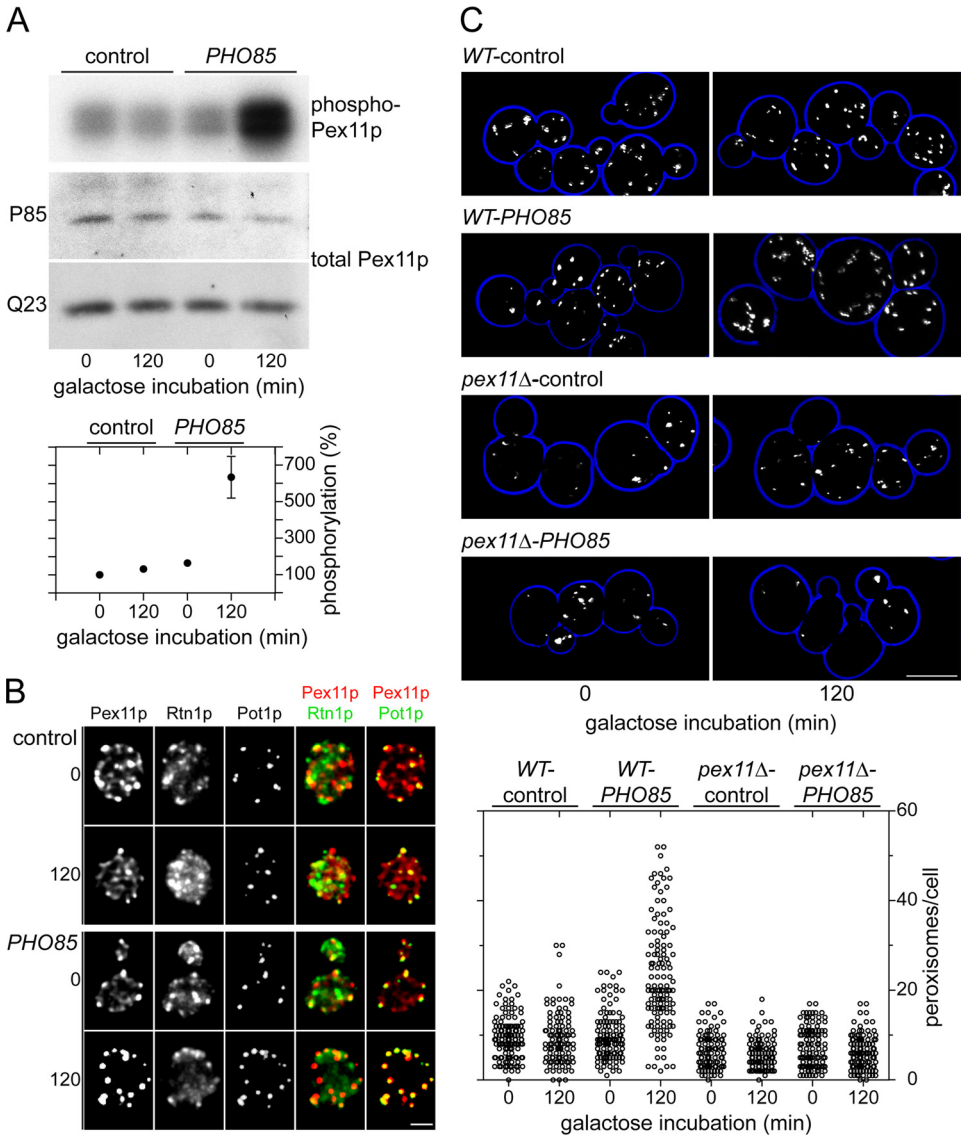


FIGURE 7. **Pho85p acts on the Pex11p-dependent pathway of peroxisome proliferation.** *A*, overexpression of the *PHO85* gene leads to increased Pex11p phosphorylation. Wild-type yeast cells harboring either a control plasmid or a *PHO85* overexpression plasmid were grown for 15 h in SCIM in the presence of 10 $\mu$Ci/ml [$^{32}$P]orthophosphate, and peroxisomal fractions were isolated before or 2 h after the addition of galactose to a final concentration of 0.5% to induce gene expression. Pex11p was immunoprecipitated from the peroxisomal fractions as described in the legend to Fig. 1. Depicted are phosphorylated (*top panel*, autoradiogram) and total Pex11p (*middle* and *bottom panels*, immunoblots) present in the immunoprecipitates. Quantification of Pex11p phosphorylation was performed from two independent experiments as described in the legend to Fig. 1. *B*, localization of Pex11p in cells overexpressing the *PHO85* gene. The intracellular distribution of Pex11p relative to the cortical ER marker Rtn1p and the peroxisomal marker Pot1p was visualized by immunofluorescence microscopy as described in the legend to Fig. 6 using anti-Pex11p antibody P85 for the detection of Pex11p. Depicted are cells at 0 and 120 min after the galactose addition. *Bar*, 2 $\mu$m. *C*, the peroxisome population is altered in cells overexpressing *PHO85*. Peroxisome morphologies were visualized by confocal fluorescence microscopy, and peroxisome numbers were determined as described in the legend to Fig. 5 in wild-type (*WT*) and *pex11*Δ cells expressing either control or *PHO85* overexpression plasmids at 0 and 120 min after the galactose addition. *Bar*, 5 $\mu$m.

be newly synthesized and is also not degraded when cells are transferred from oleate to glucose medium, we conclude that translocation of preexisting Pex11p and not newly made Pex11p accounts for the changes in Pex11p intracellular distribution.

*Overproduction of the Kinase Pho85p Leads to Hyperphosphorylation of Pex11p, Its Recruitment to Peroxisomes, and Peroxisome Proliferation*—In an attempt to identify the kinase phosphorylating Pex11p *in vivo*, we queried a library of nonessential kinase gene deletion strains (31) for mutants that contained significantly reduced levels of Pex11p as detected by immunoblotting with antibody Q8. We reasoned that although this antibody is not phosphorylation-specific, its preferential recognition of the Pex11D form of Pex11p could enable the identification of a kinase deletion mutant in which the phosphorylation of Pex11p is compromised. Only one deletion strain, *pho85*Δ, fulfilled the requirement of oleate-induced transcriptional up-regulation of the *PEX11* gene together with lack of recognition of Pex11p by antibody Q8 (supplemental Fig. S2), making Pho85p a prime candidate for a kinase acting in a signaling pathway leading to the phosphorylation of Pex11p at Ser$^{165}$ and/or Ser$^{167}$ in cells.

We assayed the effects of overexpression of the *PHO85* gene on Pex11p phosphorylation, its intracellular distribution, and peroxisome population control. When Pho85p was overproduced from a high copy number plasmid in cells containing peroxisomes induced by the presence of oleate in the medium, the concentration of Pex11p did not change (data not shown). To monitor Pho85p-induced changes in the phosphorylation of Pex11p, we performed metabolic *in vivo* labeling of wild-type cells with [$^{32}$P]orthophosphate in SCIM, as described for Fig. 1, and immunoprecipitation of Pex11p from enriched peroxisomal fractions isolated from cells before or after galactose induction of a control plasmid or a *PHO85* overexpression plasmid (Fig. 7*A*). Phosphorylation of Pex11p was strongly increased from its basal level 2 h after overexpression of Pho85p (Fig. 7*A*). We compared the intracellular distribution of Pex11p in cells before and after Pho85p overexpression. We observed a dual localization of Pex11p to punctate and reticular structures in cells prior to overexpression of Pho85p, which is consistent with the results obtained for localization of Pex11p in SCIM-grown wild-type cells (Fig. 6*A*). After overexpression of Pho85p, the Pex11p signal became concentrated in punctate structures that overlapped Pot1p-positive structures (Fig. 7*B*). The addition of galactose by itself did not elicit a relocalization of Pex11p, because Pex11p distribution remained unchanged in

cells containing the control plasmid (Fig. 7*B*). Finally, we investigated the effect of overexpressing the *PHO85* gene on cellular peroxisome populations. Increased levels of Pho85p led to elongation and proliferation of peroxisomes (Fig. 7*C*). This effect was Pex11p-dependent because no changes to peroxisome morphology and numbers were noted upon overproduction of Pho85p in a *pex11*Δ strain (Fig. 7*C*). Collectively, these data suggest that Pho85p acts in a pathway that leads to phosphorylation-induced activation of Pex11p in peroxisome division.

## DISCUSSION

Biological systems use regulatory networks, such as kinase/phosphatase signaling, to rapidly integrate a multitude of individual sensory input events into a coordinated biological response. We are investigating a role for phosphorylation in the peroxisome biogenic program and have previously reported the results of a global analysis of signaling pathways regulating fatty acid-inducible gene expression and peroxisome assembly (31, 32). In that study, yeast strains individually deleted for 249 kinases and phosphatases were evaluated for the production of a peroxisomal reporter as a transcriptional readout for nutrient-induced changes in gene expression as well as for changes in peroxisome morphology and metabolic functionality. The study enabled the delineation of several pathways involved in early and late events of peroxisome biogenesis and established a framework for a more focused analysis of how phosphorylation/dephosphorylation controls the activity of individual peroxins to dynamically modulate the peroxisomal compartment.

Here we describe a mechanism for the adjustment of cellular peroxisome populations by phosphorylation-dependent regulation of Pex11p. An analysis of antagonistic phosphomimicking mutants of Pex11p showed that the phenotypes of cells expressing these mutant forms of Pex11p resemble those of *PEX11* gene overexpression and knock-out strains (15, 16), with hyperproliferated and small peroxisomes present in cells expressing Pex11Dp and enlarged and clustered peroxisomes found in cells expressing Pex11Ap, respectively. However, the phosphomimicking mutant forms of Pex11p exert their effects on the number and size of peroxisomes in a strictly posttranscriptional manner. Our data confirm previous studies showing that Pex11p acts on peroxisome numbers and expand our understanding of the control of peroxisome dynamics by adding another layer of regulation to this process (*i.e.* the posttranslational modification of Pex11p) in addition to the previously established regulation of transcription of the *PEX11* gene.

How might phosphorylation of Pex11p control cellular peroxisome abundance? We envision that within a given cell, dephosphorylated and phosphorylated forms of Pex11p coexist in a dynamic flux. The functional differences between these Pex11p species became evident after locking them in their phosphorylation state in the phosphomimicking mutants. A striking property of Pex11Ap and Pex11Dp is their constitutive association with mature and proliferating peroxisomes, respectively. Wild-type Pex11p, in contrast, translocates between the ER and peroxisomes in a phosphorylation-dependent manner. Phosphorylation- and multimerization-controlled anterograde transport of membrane proteins in the secretory pathway has been demonstrated (33). Despite the fact that no canonical ER targeting signals have been identified in Pex11p, its ability to multimerize (34) and its modification by phosphorylation as we report here make Pex11p an optimum candidate for this type of protein trafficking. Although our findings do not preclude the conventionally accepted role for Pex11p in the division of mature peroxisomes (35), our observations also place Pex11p at an early step of peroxisome biogenesis at the interface between ER and peroxisomes. A recent report of the dual localization of Pex30p and Pex31p, which putatively act late in peroxisome biogenesis to control peroxisome size and number, to ER and peroxisomes (36) has challenged the view that these proteins act exclusively post-ER to control peroxisome dynamics. Our data suggest that the dynamic association of Pex11p with both compartments may be a prerequisite for balanced peroxisome formation. Determination of how the positioning of Pex11p in the secretory pathway mechanistically controls peroxisome abundance awaits further experimentation. However, a regulatory function for the multicompartmentalization of PMPs is becoming apparent. The storage of peroxins in the ER and their translocation to peroxisomes in response to specific signaling events as shown here for Pex11p can provide the cell with the ability to modulate the peroxisomal compartment rapidly and flexibly in response to changing internal and external conditions. Taken together, our findings provide further evidence that peroxisomal membrane proteins originate at the ER and that peroxisomes thus represent one of the many branches of the secretory pathway (37–39).

Involvement of the multifunctional kinase Pho85p in a pathway leading to increased Pex11p phosphorylation suggests that distinct signaling events converge on Pex11p. Pho85p binds multiple cyclins (40) and via activation of Pex11p may thus provide a previously suggested link (41) between cell cycle progression and peroxisome division. Another important function of Pho85p lies in the repression of stress responses. Pho85p is active and phosphorylates numerous target proteins when environmental conditions are optimal (42), which may explain the increased level of Pex11p phosphorylation in rich glucose medium. We envision that Pho85p-mediated phosphorylation of Pex11p may also lead to its exit from the ER, its association with peroxisomes, and its subsequent degradation by pexophagy. Whether Pex11p is additionally targeted by other, Pho85p-independent signaling pathways remains to be determined.

Our previous study of global kinase function (31) and this current study of the phosphorylation-dependent modulation of Pex11p have begun to define the role that phosphorylation plays in controlling peroxisome biogenesis. For the first time, we have shown how phosphorylation can activate a peroxin to regulate peroxisome dynamics. Our ultimate goal is a comprehensive understanding of the signaling mechanisms governing the formation, maintenance, and inheritance of the peroxisome.

*Acknowledgments—We thank Dr. Andrei Fagarasanu for critical reading of the manuscript, Dr. Tadashi Makio for helpful suggestions, Dr. Xuejun Sun for help with image analysis, Fred Mast for help in statistical analysis, and members of the Rachubinski laboratory for discussions. The expert technical assistance of Richard Poirier, Elena Savidov, Hanna Kroliczak, and Dwayne Weber is gratefully acknowledged.*

## REFERENCES


1. Titorenko, V. I., and Rachubinski, R. A. (2001) *Nat. Rev. Mol. Cell Biol.* **2,** 357–368
2. Gurvitz, A., and Rottensteiner, H. (2006) *Biochim. Biophys. Acta* **1763,** 1392–1402
3. Hoepfner, D., Schildknegt, D., Braakman, I., Philippsen, P., and Tabak, H. F. (2005) *Cell* **122,** 85–95
4. Tam, Y. Y., Fagarasanu, A., Fagarasanu, M., and Rachubinski, R. A. (2005) *J. Biol. Chem.* **280,** 34933–34939
5. Platta, H. W., and Erdmann, R. (2007) *FEBS Lett.* **581,** 2811–2819
6. Fujiki, Y., Matsuzono, Y., Matsuzaki, T., and Fransen, M. (2006) *Biochim. Biophys. Acta* **1763,** 1639–1646
7. Titorenko, V. I., Chan, H., and Rachubinski, R. A. (2000) *J. Cell Biol.* **148,** 29–44
8. Fagarasanu, A., Fagarasanu, M., and Rachubinski, R. A. (2007) *Annu. Rev. Cell Dev. Biol.* **23,** 321–344
9. Schrader, M., and Fahimi, H. D. (2006) *Int. Rev. Cytol.* **255,** 237–290
10. Thoms, S., and Erdmann, R. (2005) *FEBS J.* **272,** 5169–5181
11. Schrader, M., Reuber, B. E., Morell, J. C., Jimenez-Sanchez, G., Obie, C., Stroh, T. A., Valle, D., Schroer, T. A., and Gould, S. J. (1998) *J. Biol. Chem.* **273,** 29607–29614
12. Hoepfner, D., van den Berg, M., Philippsen, P., Tabak, H. F., and Hettema, E. H. (2001) *J. Cell Biol.* **155,** 979–990
13. Barnett, P., Tabak, H. F., and Hettema, E. H. (2000) *Trends Biochem. Sci.* **25,** 227–228
14. Karpichev, I. V., and Small, G. M. (1998) *Mol. Cell Biol.* **18,** 6560–6570
15. Erdmann, R., and Blobel, G. (1995) *J. Cell Biol.* **128,** 509–523
16. Marshall, P. A., Krimkevich, Y. I., Lark, R. H., Dyer, J. M., Veenhuis, M., and Goodman, J. M. (1995) *J. Cell Biol.* **129,** 345–355
17. Ptacek, J., Devgan, G., Michaud, G., Zhu, H., Zhu, X., Fasolo, J., Guo, H., Jona, G., Breitkreutz, A., Sopko, R., McCartney, R. R., Schmidt, M. C., Rachidi, N., Lee, S. J., Mah, A. S., Meng, L., Stark, M. J., Stern, D. F., De Virgilio, C., Tyers, M., Andrews, B., Gerstein, M., Schweitzer, B., Predki, P. F., and Snyder, M. (2005) *Nature* **438,** 679–684
18. Rikova, K., Guo, A., Zeng, Q., Possemato, A., Yu, J., Haack, H., Nardone, J., Lee, K., Reeves, C., Li, Y., Hu, Y., Tan, Z., Stokes, M., Sullivan, L., Mitchell, J., Wetzel, R., Macneill, J., Ren, J. M., Yuan, J., Bakalarski, C. E., Villen, J., Kornhauser, J. M., Smith, B., Li, D., Zhou, X., Gygi, S. P., Gu, T. L., Polakiewicz, R. D., Rush, J., and Comb, M. J. (2007) *Cell* **131,** 1190–1203
19. Storici, F., and Resnick, M. A. (2006) *Methods Enzymol.* **409,** 329–345
20. Fagarasanu, A., Mast, F. D., Knoblach, B., Jin, Y., Brunner, M. J., Logan, M. R., Glover, J. N., Eitzen, G. A., Aitchison, J. D., Weisman, L. S., and Rachubinski, R. A. (2009) *J. Cell Biol.* **186,** 541–554
21. Eitzen, G. A., Szilard, R. K., and Rachubinski, R. A. (1997) *J. Cell Biol.* **137,** 1265–1278
22. Weibel, E. R., and Bolender, P. (1973) in *Principles and Techniques of Electron Microscopy* (Hayat, M. A., ed) Vol. 3, pp. 237–296, Van Nostrand Reinhold, New York
23. Nonet, M., Scafe, C., Sexton, J., and Young, R. (1987) *Mol. Cell Biol.* **7,** 1602–1611
24. Tedrick, K., Trischuk, T., Lehner, R., and Eitzen, G. (2004) *Mol. Biol. Cell* **15,** 4609–4621
25. Fagarasanu, A., Fagarasanu, M., Eitzen, G. A., Aitchison, J. D., and Rachubinski, R. A. (2006) *Dev. Cell* **10,** 587–600
26. Hampton, R. Y., and Rine, J. (1994) *J. Cell Biol.* **125,** 299–312
27. Smith, J. J., Marelli, M., Christmas, R. H., Vizeacoumar, F. J., Dilworth, D. J., Ideker, T., Galitski, T., Dimitrov, K., Rachubinski, R. A., and Aitchison, J. D. (2002) *J. Cell Biol.* **158,** 259–271
28. Hu, Y., Rolfs, A., Bhullar, B., Murthy, T. V., Zhu, C., Berger, M. F., Camargo, A. A., Kelley, F., McCarron, S., Jepson, D., Richardson, A., Raphael, J., Moreira, D., Taycher, E., Zuo, D., Mohr, S., Kane, M. F., Williamson, J., Simpson, A., Bulyk, M. L., Harlow, E., Marsischky, G., Kolodner, R. D., and LaBaer, J. (2007) *Genome Res.* **17,** 536–543
29. Einerhand, A. W., Voorn-Brouwer, T. M., Erdmann, R., Kunau, W. H., and Tabak, H. F. (1991) *Eur. J. Biochem.* **200,** 113–122
30. Purdue, P. E., and Lazarow, P. B. (2001) *Annu. Rev. Cell Dev. Biol.* **17,** 701–752
31. Saleem, R. A., Knoblach, B., Mast, F. D., Smith, J. J., Boyle, J., Dobson, C. M., Long-O'Donnell, R., Rachubinski, R. A., and Aitchison, J. D. (2008) *J. Cell Biol.* **181,** 281–292
32. Rout, M. P. (2008) *J. Cell Biol.* **181,** 185–187
33. Mrowiec, T., and Schwappach, B. (2006) *Biol. Chem.* **387,** 1227–1236
34. Marshall, P. A., Dyer, J. M., Quick, M. E., and Goodman, J. M. (1996) *J. Cell Biol.* **135,** 123–137
35. Platta, H. W., and Erdmann, R. (2007) *Trends Cell Biol.* **17,** 474–484
36. Yan, M., Rachubinski, D. A., Joshi, S., Rachubinski, R. A., and Subramani, S. (2008) *Mol. Biol. Cell* **19,** 885–898
37. Schekman, R. (2005) *Cell* **122,** 1–2
38. Titorenko, V. I., and Mullen, R. T. (2006) *J. Cell Biol.* **174,** 11–17
39. Tabak, H. F., van der Zand, A., and Braakman, I. (2008) *Curr. Opin. Cell Biol.* **20,** 393–400
40. Measday, V., Moore, L., Retnakaran, R., Lee, J., Donoviel, M., Neiman, A. M., and Andrews, B. (1997) *Mol. Cell Biol.* **17,** 1212–1223
41. Yan, M., Rayapuram, N., and Subramani, S. (2005) *Curr. Opin. Cell Biol.* **17,** 376–383
42. Huang, D., Friesen, H., and Andrews, B. (2007) *Mol. Microbiol.* **66,** 303–314
43. Giaever, G., Chu, A. M., Ni, L., Connelly, C., Riles, L., Véronneau, S., Dow, S., Lucau-Danila, A., Anderson, K., André, B., Arkin, A. P., Astromoff, A., El-Bakkoury, M., Bangham, R., Benito, R., Brachat, S., Campanaro, S., Curtiss, M., Davis, K., Deutschbauer, A., Entian, K. D., Flaherty, P., Foury, F., Garfinkel, D. J., Gerstein, M., Gotte, D., Güldener, U., Hegemann, J. H., Hempel, S., Herman, Z., Jaramillo, D. F., Kelly, D. E., Kelly, S. L., Kötter, P., LaBonte, D., Lamb, D. C., Lan, N., Liang, H., Liao, H., Liu, L., Luo, C., Lussier, M., Mao, R., Menard, P., Ooi, S. L., Revuelta, J. L., Roberts, C. J., Rose, M., Ross-Macdonald, P., Scherens, B., Schimmack, G., Shafer, B., Shoemaker, D. D., Sookhai-Mahadeo, S., Storms, R. K., Strathern, J. N., Valle, G., Voet, M., Volckaert, G., Wang, C. Y., Ward, T. R., Wilhelmy, J., Winzeler, E. A., Yang, Y., Yen, G., Youngman, E., Yu, K., Bussey, H., Boeke, J. D., Snyder, M., Philippsen, P., Davis, R. W., and Johnston, M. (2002) *Nature* **418,** 387–391